Sensor Planning for Model-Based Acoustic Source Identification

Luke Calkins, Reza Khodayi-mehr, Wilkins Aquino, and Michael M. Zavlanos

***Abstract*—In this paper we propose an online active sensor planning strategy for model-based acoustic source identification (SI) in non-convex domains utilizing the three-dimensional Helmholtz partial differential equation (PDE). After discretizing the PDE using the finite element method, we formulate the SI problem as a PDE-constrained optimization problem. To make the solution computationally tractable, we employ proper orthogonal decomposition to reduce the dimension of the pressure field. Given a set of initial measurements, we solve the SI and sensor planning problems in a feedback loop. Specifically, given a set of measurements, we first solve the SI problem to get an estimate of the source field. We then fit a set of nonlinear basis functions to the solution in order to reduce the number of unknowns required to describe the source field. We finally utilize the Fisher information matrix (FIM) along with the current source parameter estimates to select the next best measurement location. Specifically, we choose a sequence of waypoints that sequentially maximize the minimum eigenvalue of the FIM with respect to the unknown source parameters. We present numerical and experimental results that showcase our proposed method. This work presents the first active sensor planning method for PDE-based acoustic SI that is investigated in practice.**

I. Introduction

Acoustic source identification (SI) refers to the estimation of the properties of possibly multiple acoustic sources, i.e., their location, intensity, or phase, given a set of measurements of the acoustic pressure field generated under the action of these sources. As the level of autonomy of robots increases, the auditory sense can be coupled with other sensors to provide more information about the robot's environment. These sensors have the benefit of being omnidirectional and they also work in low light scenarios and in the presence of obstacles. Applications of acoustic SI include human-robot interaction, enemy target tracking, or disaster relief to name a few.

The problem of acoustic source localization in robotics has been studied for a couple of decades. The most popular method is time difference of arrival (TDOA) with microphone arrays which allows the determination of the direction of arrival of a sound source relative to the array. TDOA has seen success in both ground robots [1] as well as aerial vehicles [2]. While TDOA methods work well for scenarios involving a single source in free field environments, they lack the ability to localize potentially multiple sources in complex environments. Methods also exist that can localize multiple sources using microphone arrays including beamforming [3] and the well-known multiple signal classification (MUSIC) algorithm [4]. In [5], a real-time implementation of MUSIC is utilized on a robot to localize human speakers in a noisy environment.

Since array-based methods tend to suffer in the presence of excessive noise and reverberation, introducing the environmental characteristics in the identification can help alleviate such challenges. Specifically, by considering the physics of the sound propagation in the environment in which the localization is performed, the mutli-path propagation and reverberation effects can be built into the method automatically. Many works exist to solve the SI problem given a set of noisy pressure measurements and a discretized finite element model using PDE-constrained optimization [6], [7]. Similarly, in [8], the authors show that non line-of-sight signals can be used to localize multiple sources behind a wall.

The results in [6]–[8] assume a static set of measurements are given. However, some measurements are more informative than others and therefore selecting an optimal set of measurements can achieve better identification error with fewer overall measurements. This is referred to as optimal experimental design. Since inverse problems (IPs) governed by PDEs are typically high-dimensional and ill posed, regularization is needed to get parameter estimates used in the sensor selection problem [9]. This often involves adopting a Bayesian framework and assuming some prior information on the field parameters to be estimated [10], [11]. However, these methods tend to be computationally and are thus not suitable for real-time implementation on a robot.

In the robotics and controls literature, mobile sensors have been proposed to solve IPs in an online fashion [12]. In this setting, a mobile robot equipped with a sensor can plan a sequence of measurements in order to achieve the best identification. Most of these methods are built around optimizing a scalar function of the Fisher information matrix (FIM) [13]. While estimating the spatial field, other metrics can also be optimized including the number of sensors and length of the trajectory [14], or the observation horizon [15].

In this work, we present the first active sensing approach to solving the acoustic SI problem using PDEs that is also demonstrated experimentally. Specifically, we first solve an ℓ_1 regularized least squares problem for a sparse discretized source field given a set of noisy complex-valued pressure measurements. Using this solution, we place simple nonlinear basis functions at potential source locations that depend on a small number of parameters. Based on this source estimate, we select the next best measurement location as the location which maximizes the minimum eigenvalue of the FIM with respect to the source parameters. We add the new measurement to the current set of measurements and resolve the ℓ_1 problem for the source estimate given the newly added information. We provide experimental results demonstrating the effectiveness

This material is based upon work supported by the National Science Foundation Graduate Research Fellowship Program under Grant No. 1644868.

Luke Calkins, Reza Khodayi-mehr, Wilkins Aquino and Michael M. Zavlanos are with the Department of Mechanical Engineering and Materials Science, Duke University, Durham, NC 27708, USA, {william.calkins, reza.khodayi.mehr, wilkins.aquino, michael.zavlanos}@duke.edu.

of our method in a cluttered environment where multi-path propagation and reverberation is present. The contributions of this work are a general formulation for acoustic SI that makes no assumptions on the underlying sources that are to be estimated. The algorithm can localize multiple correlated acoustic sources in reverberant environments, in contrast to many of the existing array-based methods. Furthermore, compared to the existing experimental-design literature, the introduction of nonlinear basis functions allows our planning algorithm to select more informative measurement locations by taking into account the most recent source estimate in an online way.

The rest of this paper is organized as follows. In Section II we define the acoustic SI problem and a computationally efficient way to solve it via proper orthogonal decomposition. In Section III we describe the dimensionality reduction of the source term and the next best measurement planning problem. We give numerical and experimental results in Section IV before concluding in Section V.

II. Acoustic Source Identification

A. Helmholtz Equation

Consider a domain of interest $\Omega \subset \mathbb{R}^{d_x}$ where d_x denotes the dimension of the domain and an acoustic source function $\bar{s} : \Omega \times [0, t_f] \to \mathbb{R}$ where $t_f > 0$ is the final time. The following PDE, known as the Helmholtz equation, predicts the complex-valued spatially-varying field in the frequency domain due to the source $\bar{s}$:

$$\nabla^2 p + \kappa^2 p + s/c^2 = 0, \tag{1}$$

where $\kappa = \omega/c$ is the wave-number given angular frequency ω and speed of sound c. Moreover, $s : \Omega \times [\omega_0, \omega_f] \to \mathbb{C}$ is the Fourier transform of $\bar{s}$ over the frequency range $[\omega_0, \omega_f]$. Given a set of boundary conditions and under a standard set of conditions, (1) has a unique solution [16].

Discretizing Ω with n grid points and applying appropriate conditions to the boundaries $\partial\Omega$ of the domain, we construct a finite element (FE) model that given the source function at a specific frequency ω, approximates the solution of (1). Particularly, let $\mathbf{A} \in \mathbb{C}^{n\times n}$ and $\mathbf{R} \in \mathbb{R}^{n\times n}$ denote the system and mass matrices obtained from the FE method, then

$$\mathbf{A}\mathbf{p} = \mathbf{R}\mathbf{s}, \tag{2}$$

where $\mathbf{p}, \mathbf{s} \in \mathbb{C}^n$ are complex vectors of nodal pressure and source functions. An approximation to the solution of (1) is obtained by interpolating $\mathbf{p}$ over Ω after solving (2).

In this paper, we are concerned with two types of boundary conditions. First, the sound-hard boundary

$$\nabla p \cdot \mathbf{n} = 0, \tag{3}$$

which is a zero-valued Neumann condition where $\mathbf{n}$ is outward unit normal to the boundary $\partial\Omega$. This boundary condition imposes that acoustic waves are perfectly reflected back into the domain and is a good approximation for rigid boundaries. The second boundary condition we are concerned with is the Sommerfeld radiation condition

$$\lim_{|\mathbf{x}|\to\infty} |\mathbf{x}| \left(\frac{\partial}{\partial |\mathbf{x}|} - ik \right) p = 0, \tag{4}$$

for $\mathbf{x} \in \Omega$. This boundary condition imposes that acoustic waves that impinge on the boundary travel off to infinity and are not reflected back into the domain. This condition is often used to model free-field domains.

B. Source Identification Problem

Consider m pressure measurements at locations $\{\mathbf{x}_k \in \Omega \,|\, 1 \le k \le m\}$ that sample the pressure field, $\bar{y}(\mathbf{x}_k, t) = \bar{p}(\mathbf{x}_k, t) + \epsilon$, where $\epsilon \sim \mathcal{N}(0, \sigma^2)$ denotes the additive Gaussian noise whose components are spatially and temporally independent and identically distributed. Taking the Fourier transform of the measurement signals and extracting the specific frequency of interest, we obtain the complex-valued measurement vector $\mathbf{y}_m \in \mathbb{C}^m$.

Problem 2.1: Given a set of m complex pressure measurements $\mathbf{y}_m$, estimate the source vector $\mathbf{s}$ such that the pressure values corresponding to $\mathbf{s}$, predicted by the Helmholtz FE model (2), are as close as possible in a least squares sense to the measurements $\mathbf{y}_m$.

We denote by $\mathbf{Q} \in \{0,1\}^{m\times n}$ the indicator matrix that specifies the mesh indices of the m measurement locations. Then, given a source vector $\mathbf{s}$, the multiplication $\mathbf{M}\mathbf{s}$ is the predicted pressure values at measurement locations where $\mathbf{M} = \mathbf{Q}\mathbf{A}^{-1}\mathbf{R} \in \mathbb{C}^{m\times n}$.

Given a frequency of interest, we can formulate the SI problem as a regularized least squares problem as follows

$$\min_{\mathbf{s}} \frac{1}{2}\langle \mathbf{M}\mathbf{s} - \mathbf{y}, \mathbf{M}\mathbf{s} - \mathbf{y}\rangle + \tau\mathcal{R}(\mathbf{s}), \tag{5}$$

where the notation $\langle \mathbf{s}, \mathbf{s}\rangle = \mathbf{s}^H\mathbf{s}$ denotes the inner-product in complex space and the superscript H denotes the complex conjugate transpose. $\mathcal{R}$ is a regularization operator that encodes structure in the source $\mathbf{s}$ which is the solution to the SI problem. In this work, we use $\mathcal{R}(\mathbf{s}) = \|\mathbf{s}\|_1$, where $\|\mathbf{s}\|_1 = \sum_i |\mathbf{s}_i|$ and $\mathbf{s}_i \in \mathbb{C}$ is the i-th component of the source vector and $|\mathbf{s}_i| = \sqrt{\Re(\mathbf{s}_i)^2 + \Im(\mathbf{s}_i)^2}$. The ℓ_1-norm is chosen because it is known to produce sparse solutions and we expect the area of the domain covered with sources to be small in comparison to the domain size, thus resulting in a sparse solution [17]. With this choice of regularization, it should be noted that (5) is a convex optimization problem.

C. Proper Orthogonal Decomposition

Since the dimension of the FE matrices is often on the order of 10^4 or larger for realistic problems, the inversion of the matrix $\mathbf{A}$ is not possible. The matrix $\mathbf{M}$ is needed to supply to an optimization solver in order to obtain a solution to the SI problem. In order to come up with a computationally tractable version of the problem, we employ Proper Orthogonal Decomposition (POD) to reduce the dimension of the space of pressure functions. POD gives a set of discretized basis functions $\mathbf{\Psi} = [\boldsymbol{\psi}_1, \ldots, \boldsymbol{\psi}_N]$ where $N \ll n$ and $\boldsymbol{\psi}_i \in \mathbb{C}^n$. We then obtain a reduced order model $\hat{\mathbf{p}} = \hat{\mathbf{A}}^{-1}\hat{\mathbf{R}}\mathbf{s}$ where $\hat{\mathbf{A}} = \mathbf{\Psi}^H\mathbf{K}\mathbf{\Psi}$ and $\hat{\mathbf{R}} = \mathbf{\Psi}^H\mathbf{R}$. Note that now, an $N \times N$ matrix inversion is performed, as opposed to $n \times n$. The pressure field at the nodes of the FE mesh can then be approximated as $\mathbf{p} = \mathbf{\Psi}\hat{\mathbf{p}}$. See [18] for details. Then, an

approximate closed-form mapping from the n dimensional $\mathbf{s}$ to the n dimensional $\mathbf{p}$ exists

$$\mathbf{p} = \hat{\mathbf{M}}\mathbf{s}, \tag{6}$$

where $\hat{\mathbf{M}} = \boldsymbol{\Psi}\hat{\mathbf{A}}^{-1}\hat{\mathbf{R}}$ is used in place of $\mathbf{M}$ in (5).

III. Active Sensor Planning

The solution of the SI problem (5) requires a set of m pressure measurements. In this section, we propose a strategy for collecting these measurements in an optimal way so that fewer measurements are used to achieve better estimation accuracies. The specific optimality index that we use is the minimum eigenvalue of the Fisher information matrix (FIM).

A. Reduction of the Source Term

In order to reduce the dimension of the planning problem, we reduce the number of parameters used to represent the source field. We do so by fitting a set of nonlinear basis functions to the n-dimensional source field. First we obtain the solution $\mathbf{s}^*$ to the n-dimensional SI problem (5). Then, the source field estimate is given by the FE basis and $\mathbf{s}^*$ as

$$s^h(\mathbf{x}) = \sum_{i}^{n} N_i(\mathbf{x}) s_i^*, \tag{7}$$

where $N_i(\mathbf{x})$ are the global finite element (FE) basis functions. We use nonlinear basis functions $g(\mathbf{x};\boldsymbol{\mu})$ to approximate (7)

$$\hat{s}(\mathbf{x}) = \sum_{i=1}^{K} \beta_i g(\mathbf{x};\boldsymbol{\mu}_i), \tag{8}$$

where $\beta_i \in \mathbb{C}$ is the intensity of basis function i. The functions $g : \Omega \times \boldsymbol{\mu} \to \mathbb{R}$ depend on the location $\mathbf{x} \in \Omega$ and parameters $\boldsymbol{\mu}$. Specifically, we choose Gaussian-like basis functions

$$g(\mathbf{x};\boldsymbol{\mu}_i) = \exp\{-\frac{1}{2\sigma_i^2}\|\mathbf{x}-\mathbf{c}_i\|^2\}. \tag{9}$$

Therefore $\boldsymbol{\mu}_i = [\mathbf{c}_i, \sigma_i]$, with $\mathbf{c}_i$ being the center location and σ_i being the characteristic length scale. We fix the centers (on a grid throughout the domain) and characteristic length scales σ_i of the basis functions g and solve a convex problem for the intensities β_i, $1 \le i \le K$

$$\min_{\boldsymbol{\beta}} \quad \frac{1}{2}\int (\mathbf{N}\mathbf{s} - \mathbf{G}\boldsymbol{\beta})^2 \, d\Omega + \frac{\lambda}{2}\|\boldsymbol{\beta}\|^2, \tag{10}$$

where $\mathbf{N} = [N_1(\mathbf{x}), N_2(\mathbf{x}), \ldots, N_n(\mathbf{x})]$ and $\mathbf{G} = [g_1(\mathbf{x};\boldsymbol{\mu}_1), g_2(\mathbf{x};\boldsymbol{\mu}_2), \ldots g_k(\mathbf{x};\boldsymbol{\mu}_K)]$ are the FE basis functions and nonlinear basis functions, respectively. The number of basis funtions K is chosen such that functions $\mathbf{G}$ sufficiently cover the domain and can reasonably approximate the source field $s^h(\mathbf{x})$. An ℓ_2 penalty is chosen to limit the total number of relevant basis functions and because it allows for a closed form solution to (10). The unique minimizer $\boldsymbol{\beta}$ of problem (10) is

$$\boldsymbol{\beta}^* = \left(\int \mathbf{G}^T\mathbf{G} \, d\Omega + \lambda\mathbf{I}\right)^{-1} \left(\int \mathbf{G}^T\mathbf{N} \, d\Omega \, \mathbf{s}^*\right). \tag{11}$$

It should be noted that the integrals $\int \mathbf{G}^T\mathbf{G} \, d\Omega \in \mathbb{R}^{K\times K}$ and $\int \mathbf{G}^T\mathbf{N} \, d\Omega \in \mathbb{R}^{n\times n}$ in (10) can be calculated offline as they only depend on the FE basis functions and the user-defined grid of basis functions $\mathbf{G}$. The basis functions g are set to zero for $\|\mathbf{x}-\mathbf{c}_i\| \ge 3\sigma_i$ where they are practically zero. This makes $\int \mathbf{G}^T\mathbf{G} \, d\Omega$ and $\int \mathbf{G}^T\mathbf{N} \, d\Omega$ sparse which speeds up the computation of $\boldsymbol{\beta}^*$. Solving (11) requires one $K \times K$ sparse linear system solve. Since $\mathbf{s}^*$ is sparse, many of the β_i's will be zero.

After fitting the nonlinear representation $\hat{s}$ to the source estimate s^h, we can sort the intensities $\boldsymbol{\beta}$ of these basis functions in descending order of magnitude and keep L basis functions of the total K defined. Specifically, for a given fraction η, we keep L basis function coefficients β_i such that

$$\frac{\sum_{i=1}^{L}|\beta_i|}{\sum_{i=1}^{K}|\beta_i|} \le \eta \tag{12}$$

where $0 < \eta < 1$ and the summation is taken over the sorted intensities. This way we eliminate basis functions that contribute very little energy to the overall source field. By eliminating these basis functions, we obtain $5L$ parameters that very efficiently describe the source field, i.e., the three-dimensional center coordinate and the two dimensional strength (real and imaginary component of β) for each basis function. The pressure field depends nonlinearly on these parameters $\boldsymbol{\theta}_i = [\mathbf{c}_i, \beta_i], 1 \le i \le L$ which are grouped together into the unknown parameter $\boldsymbol{\theta} = [\boldsymbol{\theta}_1, \ldots, \boldsymbol{\theta}_L]$. Since σ_i is fixed and the same for each basis function as given in (9), is it not considered an unknown parameter to be estimated.

B. The Sensor Planning Problem

Given an initial set of m complex-valued pressure measurements denoted by $\mathbf{y}_m = (y(\mathbf{x}_1), \ldots, y(\mathbf{x}_m))$, we solve the SI problem (5) to get an estimate of the source field. Then we construct a nonlinear representation from (11), as per the discussion in Section III-A. Assuming that the measurement noise is additive and spatially independent, i.e.

$$\mathbf{y}(\mathbf{x}_i) = p(\mathbf{x}_i) + \epsilon$$

where $\epsilon \sim \mathcal{CN}(0, \sigma_n^2)$ (complex normal distribution), the FIM is given in closed form [19]

$$\mathbf{F}_m = \frac{2}{\sigma_n^2}\sum_{i=1}^{m} \Re\left(\frac{\partial p(\mathbf{x}_i)}{\partial \boldsymbol{\theta}}^H \frac{\partial p(\mathbf{x}_i)}{\partial \boldsymbol{\theta}}\right), \tag{13}$$

where $p(\mathbf{x}_i) = \hat{\mathbf{M}}_i\hat{\mathbf{s}}(\boldsymbol{\theta})$ is given by the POD model (6). The vector $\hat{\mathbf{s}}(\boldsymbol{\theta}) \in \mathbb{C}^n$ corresponds to the function $\hat{s}$ evaluated at the nodes of the FE mesh after truncating the basis functions according to (12). $\hat{\mathbf{M}}_i$ is the i'th row of $\hat{\mathbf{M}}$ which gives the complex pressure at location $\mathbf{x}_i$ after multiplication with $\hat{\mathbf{s}}(\boldsymbol{\theta})$. In (13), $\boldsymbol{\theta} = [\boldsymbol{\theta}_1, \ldots, \boldsymbol{\theta}_L]$ encompasses all the unknown parameters for each source basis function kept (including the β's); see section III-A for details.

Since $\hat{\mathbf{M}}$ is constant, $\partial p/\partial\boldsymbol{\theta} = \hat{\mathbf{M}}\partial\mathbf{s}/\partial\boldsymbol{\theta}$, where $\partial\mathbf{s}/\partial\boldsymbol{\theta}$ is the derivative of (8) evaluated at the mesh nodes (one entry for each mesh coordinate). We are representing the nonlinear source function and its gradient with respect to $\boldsymbol{\theta}$ in the FE

Algorithm 1 Active Sensor Planning Algorithm

Require: Set of POD basis functions $[\psi_1, \ldots, \psi_N]$;
Require: Initial number of measurements m_{init} and maximum number of measurements m_{max};
Collect the initial measurement locations $\tilde{\mathbf{x}}^{m_{\text{init}}} = (\mathbf{x}_1, \ldots, \mathbf{x}_{m_{\text{init}}})$ and corresponding measurements $\tilde{\mathbf{y}}_{m_{\text{init}}} = (\mathbf{y}(\mathbf{x}_1), \ldots, \mathbf{y}(\mathbf{x}_{m_{\text{init}}}))$;
for $m = m_{\text{init}}$ **to** $m = m_{\text{max}}$ **do**
  Solve (5) with $\tilde{\mathbf{y}}_m$ and $\hat{\mathbf{M}}$ to get $\mathbf{s}^*_m$;
  Fit nonlinear representation (11) to get $\boldsymbol{\beta}^*_m$;
  Sort $\boldsymbol{\beta}^*_m$ and truncate according to (12);
  Form $\mathbf{F}_m$ according to (13) using $\tilde{\mathbf{x}}^m$ and truncated $\boldsymbol{\beta}^*_m$;
  Solve next best measurement problem (15) for $\mathbf{x}_{m+1}$;
  Update waypoints $\tilde{\mathbf{x}}^{m+1} = (\tilde{\mathbf{x}}^m, \mathbf{x}_{m+1})$;
  Update measurement set $\tilde{\mathbf{y}}_{m+1} = (\tilde{\mathbf{y}}_m, \mathbf{y}(\mathbf{x}_{m+1}))$;
  $m \leftarrow m + 1$;
end for

basis. Taking the derivative of each entry of the vector $\hat{\mathbf{s}}(\mathbf{x}; \boldsymbol{\theta})$ with respect to $\boldsymbol{\theta}$ as

$$\frac{\partial \hat{\mathbf{s}}}{\partial \boldsymbol{\theta}} = \frac{\partial}{\partial \boldsymbol{\theta}} \begin{bmatrix} \hat{s}(\mathbf{x}_1; \boldsymbol{\theta}) \\ \hat{s}(\mathbf{x}_2; \boldsymbol{\theta}) \\ \vdots \\ \hat{s}(\mathbf{x}_n; \boldsymbol{\theta}) \end{bmatrix} = \begin{bmatrix} \partial \hat{s}/\partial \boldsymbol{\theta}(\mathbf{x}_1; \boldsymbol{\theta}) \\ \partial \hat{s}/\partial \boldsymbol{\theta}(\mathbf{x}_2; \boldsymbol{\theta}) \\ \vdots \\ \partial \hat{s}/\partial \boldsymbol{\theta}(\mathbf{x}_n; \boldsymbol{\theta}) \end{bmatrix}, \qquad (14)$$

the FIM (13) can then be calculated.

Specifically, we create a set of candidate measurement locations in the domain Ω, collected in the set $\mathcal{E}$. Then, the sensor planning problem is to select the next best measurement location so as to maximize the minimum eigenvalue of the FIM, i.e.,

$$\mathbf{x}^{m+1} = \underset{\mathbf{x} \in \mathcal{E}}{\text{argmax}} \quad \lambda_{\text{min}} \left[\mathbf{F}_m + \frac{\partial \hat{\mathbf{s}}}{\partial \boldsymbol{\theta}}^H \hat{\mathbf{M}}_i^H \hat{\mathbf{M}}_i \frac{\partial \hat{\mathbf{s}}}{\partial \boldsymbol{\theta}} \right], \qquad (15)$$

where $\hat{\mathbf{M}}_i$ is the only term that depends on the measurement location $\mathbf{x}$. In the experiment design literature, this is referred to as the E-optimal design and translates to minimizing the worst case error of the parameters. Once the next measurement is added to the set of measurements, the SI problem (5) is solved again, followed by a new nonlinear source parametrization. Then, a new waypoint is selected, and the process repeats. The described algorithm is summarized in Algorithm 1.

Remark 3.1: If we treated the source nodal values s^*_i, $1 \leq i \leq n$ as the parameters that we want to maximize a scalar measure of the FIM with respect to, then the FIM would be $n \times n$ with rank of at most m since each term in the summation of (13) is rank 1. Furthermore, after taking the derivatives in (13), the values of the source parameters do not affect the FIM, because $\partial/\partial \mathbf{s}(\hat{\mathbf{M}}_i \mathbf{s}) = \hat{\mathbf{M}}$. Therefore, the FIM does not depend on the current estimate of the source and there is no need for online planning. The nonlinear fitting of the n dimensional field helps to reduce the size of the planning problem as well as making use of current information.

Remark 3.2: Note that the proposed ℓ_1 regularization in (5) produces bias that depends on the unknown parameters that are being estimated and the regularization parameters. Exact expressions for the bias in ℓ_1 regularization are difficult to get. In some inverse problems the bias is the most important component of the overall uncertainty. To address bias, we are currently exploring ways to control the mean squared error (MSE), not just the variance captured by the FIM. Since the MSE depends on the unknown parameters, we can use a prior distribution on the parameters to control the average MSE.

IV. Results

A. Two Source Numerical Experiment

We present numerical simulations of Algorithm 1 being executed in a domain with a reflecting surface on one side of the domain as well as a wall placed in the middle of the domain that also acts as an acoustic reflecting surface. The sound hard boundary condition (3) is applied to the reflecting surfaces and the Sommerfeld radiation condition (4) to all other boundaries. The finite element (FE) matrices (2) are constructed using an in-house FE code. The dimensions of the computational domain are $2.2 \times 0.55 \times 2.7$ meters. To simulate two sources, two nodes in the FE mesh corresponding to the two source locations are given equal non-zero values, i.e., the vector $\mathbf{s}$ in (2) has two non-zero entries. In this case, the sources are radiating in phase as acoustic monopoles and therefore radiate acoustic energy equally in all directions. Therefore, the sources are perfectly correlated and many array-based methods would have difficulty calculating the direction of arrival of either source signal. A frequency of $f = 400$ Hz is chosen and utilized in (2) to generate the pressure data and 20% measurement noise is artificially added to the simulated pressure values. Algorithm 1 is initialized with $m_{\text{init}} = 32$ measurements and $m_{\text{max}} = 42$ total measurements such that 10 additional measurements are added during the execution of the algorithm. Regularization values of $\tau = 1 \times 10^{-6}$ in (5), and $\lambda = 1 \times 10^{-10}$ in (11) were utilized as these values worked well for this domain over several simulation studies. The parameter η in (12) was set to 0.9, i.e., 90% of the total source field energy was kept in the nonlinear fitting. The planning measurements selected, along with the initial measurements for the two source simulation can be seen in Figure 1. The planning algorithm tends to pick measurements close to higher peaks in the current estimate of the source field. A 3D plot of the magnitude of the final estimated source field can be seen in Figure 2. Only those nodes in the FE mesh with 50% of the magnitude of the maximum magnitude node are depicted. We estimate the source centers to be located as these active nodes. The localization error for the source in the top right of Figure 2 is approximately 11.2 cm and approximately 7.9 cm for the one in the lower part of Figure 2.

B. Experimental Setup

To illustrate our proposed method experimentally, we test our algorithm inside an anechoic chamber. This is an enclosed space with foam cones lining the walls that act as sound absorbers, simulating a free-field environment. We constructed the same domain used in the simulations in the previous section. We placed two MDF wood panels within the domain

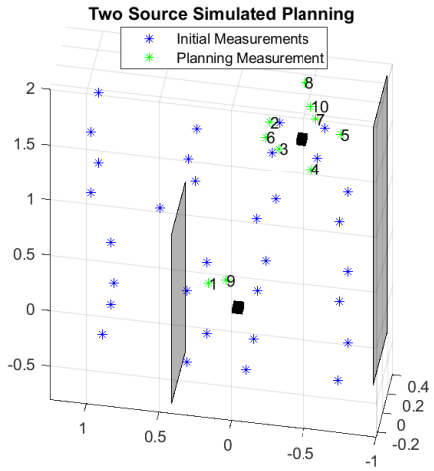

Fig. 1: Planning measurement sequence for two source simulated case. Sources are depicted by the black cubes. Domain dimensions in meters.

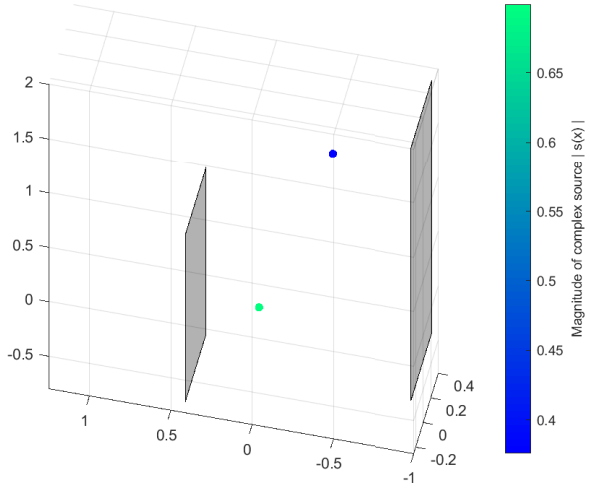

Fig. 2: Final source field estimate, displayed as magnitude of complex-valued field where 50% thresholding is applied.

that act as acoustic reflectors due to their high density and rigidity. An Optimus XTS-40 speaker was utilized as the acoustic source. Time harmonic fields are generated by driving the speaker with a mixture of pure tones of different phase ranging in frequency from 200 Hz - 1000 Hz in intervals of 50 Hz. Pressure measurements are collected using 4 PCB Piezotronics pre-polarized half-inch microphones, model 377B02. The microphones and speaker are controlled using a Data Translation DT9857E signal conditioning board. The setup can be seen in Figure 3.

Since we are not able to move a robot in 3D in the chamber, we collect measurements a priori and store them in the set $\mathcal{E}$. Then, using Algorithm 1, we select the most informative measurements from the set $\mathcal{E}$, one by one, and use those currently collected to update the estimate of the source. To collect the measurements in the set $\mathcal{E}$, since we only have four microphones available, we run many experimental trials with the microphones in different locations. Specifically, we send

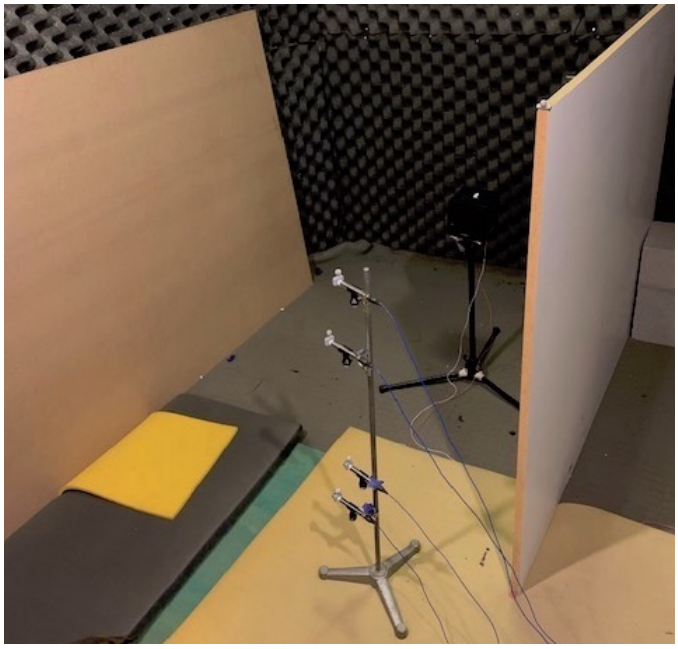

Fig. 3: Experimental setup with speaker placed in between the two reflecting wood surfaces. The four microphones can also be seen on the stand.

the same driving signal to the speaker for each trial and remove the same two-second time slice from each microphone thus synchronizing the recorded signals in time across all trials.

Since the SI problem is solved using complex pressure measurements in the frequency domain, both the magnitude and phase at each measurement location is crucial to solving the SI problem (5). Therefore, without the time synchronization of the measurements across the different trials, the phase information at the different measurements would be incorrect. If the experiment were run using a mobile robot, it cannot take measurements at different locations simultaneously, therefore a stationary microphone would be necessary that takes measurements continuously and provides the robot with the appropriate phase shift to apply to each of its measurements. The microphone acts as ground truth and helps achieve the same time synchronization between measurements.

C. Experimental Results

We present here an experiment involving a single source placed in between the two MDF wood panels in the chamber. The sound-hard boundary condition (3) is applied to the two wood panels and the Sommerfeld radiation condition (4) is applied to all other boundaries of the domain. This experiment is run at $f = 500$ Hz to remain above the anechoic cutoff limit of the chamber. The algorithm is initialized with $m_{\text{init}} = 24$ exploration measurements placed on a uniform grid throughout the domain. A total of 10 measurements are selected from the set $\mathcal{E}$ and added to the initial set, making $m_{\text{max}} = 34$. The sequence of the measurements can be seen in Figure 4.

The final estimated source field can be seen in Figure 5. Only those nodes within 50% of the magnitude of the maximum node are depicted. Since there are multiple active nodes clustered together, in order to estimate the source

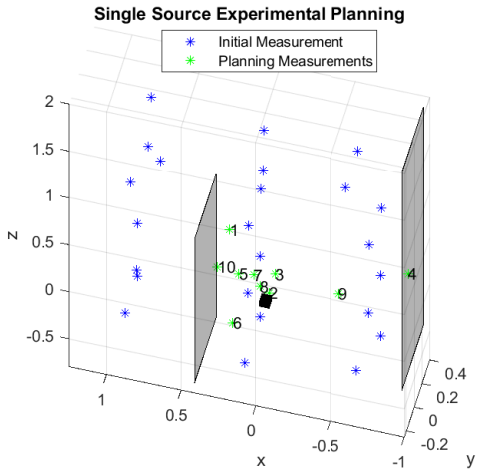

Fig. 4: Measurement sequence for single source experiment.

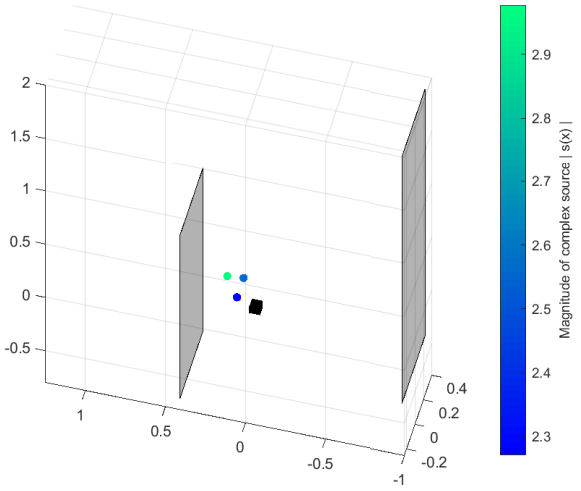

Fig. 5: Final thresholded source field. Source depicted as black cube.

location, we took the weighted average of the location of these active nodes, weighted by the complex magnitude at each node. The localization error was approximately 34 cm.

V. Conclusion

In this paper we proposed an active sensor planning strategy to identify arbitrary acoustic source fields in complex domains. We formulated the problem as a convex regularized least squares problem subject to the Helmholtz partial differential equation. Given an initial set of noisy complex-valued pressure measurements, we presented an algorithm to sequentially select the next best measurement in order to estimate the source field. This was achieved by reducing the order of the finite element model as well as reducing the number of parameters used to describe the source field. The measurement waypoints were selected so as to maximize the minimum eigenvalue of the Fisher information matrix with respect to the reduced set of source parameters. We illustrated our algorithm in numerical simulations as well as real-world experiments.

References

[1] J.-M. Valin, F. Michaud, J. Rouat, and D. Létourneau, "Robust sound source localization using a microphone array on a mobile robot," in *Intelligent Robots and Systems, Proceedings. IEEE/RSJ International Conference on*, vol. 2, pp. 1228–1233, IEEE, 2003.

[2] M. Basiri, F. Schill, P. U. Lima, and D. Floreano, "Robust acoustic source localization of emergency signals from micro air vehicles," in *Intelligent Robots and Systems (IROS), 2012 IEEE/RSJ International Conference on*, pp. 4737–4742, IEEE, 2012.

[3] J.-M. Valin, F. Michaud, B. Hadjou, and J. Rouat, "Localization of simultaneous moving sound sources for mobile robot using a frequency-domain steered beamformer approach," in *Robotics and Automation, 2004. Proceedings. ICRA'04. 2004 IEEE International Conference on*, vol. 1, pp. 1033–1038, IEEE, 2004.

[4] R. Schmidt, "Multiple emitter location and signal parameter estimation," *IEEE Transactions on Antennas and Propagation*, vol. 34, no. 3, pp. 276–280, 1986.

[5] C. T. Ishi, O. Chatot, H. Ishiguro, and N. Hagita, "Evaluation of a music-based real-time sound localization of multiple sound sources in real noisy environments," Institute of Electrical and Electronics Engineers, 2009.

[6] I. Dokmanić and M. Vetterli, "Room helps: Acoustic localization with finite elements," in *Acoustics, Speech and Signal Processing, IEEE International Conference on*, pp. 2617–2620, IEEE, 2012.

[7] L. Calkins, R. Khodayi-mehr, W. Aquino, and M. M. Zavlanos, "Physics-based acoustic source identification," in *2018 IEEE Conference on Decision and Control (CDC)*, pp. 1457–1462, IEEE, 2018.

[8] S. Kitic, N. Bertin, and R. Gribonval, "Hearing behind walls: localizing sources in the room next door with cosparsity," in *Acoustics, Speech and Signal Processing, IEEE International Conference on*, pp. 3087–3091, IEEE, 2014.

[9] L. Tenorio, C. Lucero, V. Ball, and L. Horesh, "Experimental design in the context of Tikhonov regularized inverse problems," *Statistical Modelling*, vol. 13, no. 5-6, pp. 481–507, 2013.

[10] J. Yu, V. M. Zavala, and M. Anitescu, "A scalable design of experiments framework for optimal sensor placement," *Journal of Process Control*, vol. 67, pp. 44–55, 2018.

[11] A. Alexanderian, N. Petra, G. Stadler, and O. Ghattas, "A-optimal design of experiments for infinite-dimensional Bayesian linear inverse problems with regularized ℓ_0-sparsification," *SIAM Journal on Scientific Computing*, vol. 36, no. 5, pp. A2122–A2148, 2014.

[12] R. Khodayi-mehr, W. Aquino, and M. M. Zavlanos, "Model-based active source identification in complex environments," *IEEE Transactions on Robotics*, 2019.

[13] D. Ucinski, *Optimal measurement methods for distributed parameter system identification*. CRC Press, 2004.

[14] C. Tricaud, M. P. Dariusz, U. Yang, and Q. Chen, "D-optimal trajectory design of heterogeneous mobile sensors for parameter estimation of distributed systems," in *American Control Conference, 2008*, pp. 663–668, IEEE, 2008.

[15] D. Ucinski and Y. Chen, "Time–optimal path planning of moving sensors for parameter estimation of distributed systems," in *Decision and Control, 2005 and 2005 European Control Conference. CDC-ECC'05. 44th IEEE Conference on*, pp. 5257–5262, IEEE, 2005.

[16] L. E. Kinsler, A. R. Frey, A. B. Coppens, and J. V. Sanders, "Fundamentals of acoustics," *Fundamentals of Acoustics, 4th Edition, by Lawrence E. Kinsler, Austin R. Frey, Alan B. Coppens, James V. Sanders, pp. 560. ISBN 0-471-84789-5. Wiley-VCH, December 1999.*, p. 560, 1999.

[17] R. Khodayi-mehr, W. Aquino, and M. M. Zavlanos, "Model-based sparse source identification," in *American Control Conference (ACC), 2015*, pp. 1818–1823, IEEE, 2015.

[18] J. A. Atwell and B. B. King, "Proper orthogonal decomposition for reduced basis feedback controllers for parabolic equations," *Mathematical and computer modelling*, vol. 33, no. 1-3, pp. 1–19, 2001.

[19] S. M. Kay, *Fundamentals of statistical signal processing*. Prentice Hall PTR, 1993.